

AMITE: A Novel Polynomial Expansion for Analyzing Neural Network Nonlinearities

Mauro J. Sanchirico III, Xun Jiao, and C. Nataraj

Abstract—Polynomial expansions are important in the analysis of neural network nonlinearities. They have been applied thereto addressing well-known difficulties in verification, explainability, and security. Existing approaches span classical Taylor and Chebyshev methods, asymptotics, and many numerical approaches. We find that while these individually have useful properties such as exact error formulas, adjustable domain, and robustness to undefined derivatives, there are no approaches that provide a consistent method yielding an expansion with all these properties. To address this, we develop an analytically modified integral transform expansion (AMITE), a novel expansion via integral transforms modified using derived criteria for convergence. We show the general expansion and then demonstrate application for two popular activation functions, hyperbolic tangent and rectified linear units. Compared with existing expansions (i.e., Chebyshev, Taylor, and numerical) employed to this end, AMITE is the first to provide six previously mutually exclusive desired expansion properties such as exact formulas for the coefficients and exact expansion errors (Table II). We demonstrate the effectiveness of AMITE in two case studies. First, a multivariate polynomial form is efficiently extracted from a single hidden layer black-box Multi-Layer Perceptron (MLP) to facilitate equivalence testing from noisy stimulus-response pairs. Second, a variety of Feed-Forward Neural Network (FFNN) architectures having between 3 and 7 layers are range bounded using Taylor models improved by the AMITE polynomials and error formulas. AMITE presents a new dimension of expansion methods suitable for analysis/approximation of nonlinearities in neural networks, opening new directions and opportunities for the theoretical analysis and systematic testing of neural networks.

Index Terms—Neural Networks, Equivalence, Taylor, Fourier, Polynomial, Approximation.

I. INTRODUCTION

IN the design and implementation of nonlinear systems, polynomial expansions provide an important means of decomposing nonlinear functions into a form facilitating analysis. Both classical and modern neural networks have inherent nonlinearities in their activation functions such as hyperbolic tangent and rectified linear units. Various polynomial expansions and approximations have been applied to neural network activations enabling explainable, verifiable, and secure deployment of neural systems, with [1], [2], and [3] being three recent examples respectively. The motivation to develop explainability and verification techniques is further enhanced by proposed or studied use of neural networks for critical systems such as

M. Sanchirico is with the Lockheed Martin Artificial Intelligence Center, Mt Laurel Township, NJ 08054 USA and the Department of Electrical and Computer Engineering, Villanova University, Villanova PA, 19085 USA

X. Jiao is with the Department of Electrical and Computer Engineering, Villanova University, Villanova, PA, 19085 USA

C. Nataraj is with the Villanova Center for Analytics of Dynamic Systems (VCADS), Villanova University, Villanova, PA, 19085 USA

TABLE I
QUALITATIVE PROPERTIES CONSIDERED FOR A POLYNOMIAL EXPANSION OF THE FORM: $\varphi(v) = \sum_m \alpha_m v^m + H_M(v)$

Property	Description
<i>Exact Coeffs.</i>	Precise analytic equations available for the coefficients, α_m , for the nonlinearities considered.
<i>Explicit Exact Errors</i>	Precise analytic equations are explicitly worked for the expansion errors, $H_M(v)$.
<i>Monic Form</i>	The expansion is formulated directly as a sum of monomials, i.e., $\sum_m \alpha_m v^m$ and not as a sum of other polynomials or piecewise polynomials.
<i>Adjustable Domain</i>	The approximation $\varphi(v) = \sum_m \alpha_m v^m$ is valid for any desired domain of validity $ v < V$ without transforming or re-scaling v .
<i>Handles undef. derivs.</i>	The expansion is valid if some of the derivatives of φ are undefined.
<i>Consistent Method</i>	The method can be applied consistently to a wide variety of functions without ad-hoc modifications.

unmanned aerial vehicles [4], [5], hypersonic vehicles [6], or even air-to-air combat in recent work [7]. Meanwhile, use of neural networks in healthcare applications, such as [8], further drives the need for secure inference techniques to protect third party private information [3], [9]. The polynomial expansion of neural network activation functions is a method employed in addressing all of these diverse and important challenges.

The existing polynomial expansions of neural nonlinearity can be categorized as follows. First, the well-known Taylor series is employed often [1], [20]–[24]. While Taylor series provides the advantage of exact formulas for coefficients and errors and often provides a useful local approximation, its domain of validity is limited to $|v| < \frac{\pi}{2}$ for $\tanh(v)$ nonlinearities [19] and it requires that a function have defined derivatives in the expansion domain. A well-known identity for large arguments is given: $\tanh(v) = 1 + 2 \sum_{m=1}^{\infty} (-1)^m e^{-2mv} \forall v > 0$ [25], and can be manipulated into a power series like form by expanding e^{-2mv} . However, the result is still not valid for small v . Similarly, many asymptotic series are available for nonlinear functions such as \tanh but often have restricted domains (e.g., large arguments) [10], do not have a monic form, and are not generally differentiable [25].

A Chebyshev approximation can be applied using recursive formulas for the coefficients [12]. References employing Chebyshev approximations or comparing them to other approximations for neural nonlinearities include [15], [26] and [3]. Alternatively, the Fourier-Legendre series [27] has well-known methods for fast coefficient computation [14] and

TABLE II
QUALITATIVE COMPARISON OF POLYNOMIAL EXPANSION TECHNIQUES AVAILABLE FOR NEURAL NETWORK NONLINEARITIES

	<i>Exact Coeffs.</i>	<i>Explicit Exact Errors</i>	<i>Monic Form</i>	<i>Adjustable Domain</i>	<i>Handles Undef. Derivs.</i>	<i>Consistent Method</i>
AMITE	Y	Y	Y	Y	Y	Y
Asymptotics [10]	Y				Y	
Bernstein [11]	Y			Y	Y	Y
Chebyshev [12]	Y				Y	Y
Exponential Chebyshev [13]	Y			Y	Y	Y
Fast Fourier-Legendre [14]					Y	Y
Least Squares Regression [3]			Y	Y	Y	Y
Minimax w. Chebyshev [3], [15]				Y	Y	Y
Piecewise [16]				Y	Y	
Recursive Regression [2]				Y	Y	Y
Remez / Modified Remez [17], [18]				Y	Y	Y
Taylor [19]	Y	Y	Y			Y

provides a fast rate of convergence. The Bernstein basis is employed by Huang et al. in ReachNN to perform reachability analysis for neural controlled systems [11]. Overall, the related polynomial basis techniques via Chebyshev, Fourier-Legendre, Bernstein and similar methods provide accurate approximation with the useful property that formulas for coefficients can be exact using some methods. However, while most methods employing such techniques provide upper bounds on the error, exact error formulas have not yet been provided for the expansions of the neural nonlinearities considered.

If analytic formulas are not required, many numerical techniques are available to approximate a nonlinearity. Obla et al. compare least squares and best uniform approximation (i.e., minimax approximation) against Taylor series [3]. Lee et al. also use a minimax approximation with a Chebyshev basis [15], improving upon results from a modified Remez algorithm [17]. Numerically fit piecewise polynomials are suited for efficient implementation of a nonlinear function such as tanh over a wide domain [28], [29]. Piecewise approximations can be combined with other methods, e.g., Chebyshev [16].

Piecewise linear polynomials specifically are well suited to relu nonlinearities which are a special case thereof. They are key components of the Marabou framework for verification of deep neural networks [30] and employed by Dutta et al. to perform reachability analysis via regressive polynomial rule inference [2]. Dutta et al. further reduce the expansion error by repeatedly fitting a low order polynomial and fitting a new polynomial to the residual. This approach keeps the resulting polynomial order low but does not lend itself to extraction of exact error formulas, which the authors cite as a challenge and then solve by further reduction to a piecewise linear model [2].

To address the limitations of many existing polynomial approximations, we employ a special functions approach to develop a new technique, applicable to a wide class of neural network nonlinearities and having many of the desirable properties of the above expansions including many that were previously mutually exclusive. Motivated by applications noted above, we provide, for the first time, the derivation of explicit exact error formulas and useful analytic approximations

thereof. To facilitate mathematical manipulation, we provide a monic polynomial form like that of the Taylor series and an adjustable domain of convergence that does not require transformation or re-scaling. We provide exact coefficients that do not require iteration or recursion to compute and avoid the main disadvantage of the Taylor series by remaining robust to undefined derivatives. Furthermore, the method provides a consistent approach which can be readily applied to a wide variety of nonlinear functions without *ad hoc* manipulation for a specific nonlinearity type. Exploitation of these new properties is then demonstrated in the case studies that follow.

The expansion is developed using integral transforms of the generalized Fourier type, modified according to derived criteria for convergence and as such is called the analytically modified integral transform expansion (AMITE) technique. The qualitative expansion properties that we consider are defined in Table I. We present a comprehensive comparison of AMITE with existing state-of-the-art expansion methods with respect to these properties in Table II.

We summarize our contributions in this paper as follows.

- **Novel polynomial expansion and errors:** We develop a novel polynomial expansion technique, the analytically modified integral transform expansion (AMITE), via a special functions approach to enable decomposing neural network activation functions into polynomial forms having several advantageous properties, listed in Table II, many of which would otherwise be mutually exclusive. We show the general expansion method and its specific employment for the hyperbolic tangent and ReLU. Exact error formulas are derived and analyzed via exploitation of a number of non-trivial relationships amongst the special and elementary functions.
- **Black-box MLP equivalence testing example:** Using a single hidden layer MLP as a first case study, we demonstrate use of the AMITE technique in a black-box system identification based equivalency test for checking that a given MLP is output-equivalent to another from noisy stimulus-response pairs. While similar methods would require piecewise polynomials or numerical fits

due to the limitations of existing expansions available for neural nonlinearities, we show that we can efficiently expand the entire MLP as a single multivariate polynomial approximation. This is enabled by the adjustable domain of convergence and simple monic form, and is advantageous for facilitating exact error analysis.

- **Improved range bounding for deep FFNNs:** Using the problem of range bounding the output of a deep FFNN over a set of input domain intervals as a second case study, we construct an improved Taylor model representation for deep FFNNs wherein the AMITE polynomials and exact error formulas are specifically exploited to provide tighter output range bounds over larger domain intervals than possible with a conventional Taylor model (i.e., a Taylor model based on the Taylor series and its error bounds). A method for speeding up computation of the range bounds using the AMITE's analytic error approximations while retaining the rigor of exact error handling is provided for the first time. These improvements combined with the newly developed exact formulas imply that the AMITE technique is a useful complement to the existing repertoire of polynomial expansions employed in the analysis of neural systems.

Organization of the paper: Section II defines the notation. The main expansions and errors are developed in Section III and expansion results are summarized in Section IV. The case study for equivalence testing a single hidden layer MLP is presented in Section V and the case study for range bounding a deep FFNN is presented in Section VI. Related work is reviewed in Section VII and Section VIII concludes the paper.

II. DEFINITIONS AND PROBLEM FORMULATION

The hyperbolic tangent and ReLU are defined: $\tanh(v) = \frac{e^v - e^{-v}}{e^v + e^{-v}}$, $\text{relu}(v) = \frac{|v+v|}{2}$. When developing approximations of activation functions φ we denote their coefficients α_m

$$\varphi(v) \simeq \sum_{m=0}^M \alpha_m v^m. \quad (1)$$

We consider FFNNs having N_I inputs, N_L layers, and $N_H^{[l]}$ hidden neurons per layer l . We use α to denote activation function coefficients and β to denote the collection of weights and biases $\beta = \{W^{\{0\}}, \dots, W^{\{N_L\}}, b^{\{0\}}, \dots, b^{\{N_L\}}\}$ such that each network layer has the input-output relationship:

$$y(\alpha, \beta, x) = W^{\{l\}} \varphi \left(W^{\{l-1\}} x + b^{\{l-1\}} \right) + b^{\{l\}} \quad (2)$$

Linear activations are used on the last layer. The input to hidden neuron n is denoted

$$v_n = b_n^{\{l-1\}} + \sum_{i=1}^{N_I} w_{n,i}^{\{l-1\}} x_i \quad \forall n \in [1, N_H^{[l]}]. \quad (3)$$

The standard definition of a Taylor model, \mathcal{T} , due to Berz [31], [32] for a function, φ , is employed, i.e.,

$$\mathcal{T}_M^{\{\varphi\}} = \{[\alpha_m], (e_{\min}, e_{\max})\}, \quad (4)$$

where $[\alpha_m]$ and (e_{\min}, e_{\max}) denote the polynomial coefficients of φ and the rigorous error interval of the approximation. While Taylor series is usually employed to derive α ,

other polynomial approximation methods (surveyed in I) have been employed. In the second case study, AMITE and Taylor polynomials are compared for the Taylor modeling of deep FFNNs. Standard rules [31], [32] for addition, multiplication, and composition of Taylor models are employed. Interval arithmetic operations for handling errors are implemented as a simplified subset of IEEE 1788.1 [33]. We assume that nonlinearities, φ , to be analyzed can be represented by integral transforms in the form of $\varphi(v) = \int_{\mathbb{R}} \Phi(\xi) f(\xi v) d\xi$ wherein the kernels have Taylor series convergent on $(-\infty, \infty)$ of the form $f(\xi v) = \sum_{m=0}^{\infty} \tilde{f}(m)(\xi v)^m$.

III. AMITE DEVELOPMENT

To achieve the expansion properties shown in Table II for the AMITE technique we seek expressions of the forms:

$$\tanh(v) \simeq \sum_{m=0}^M T_{2m+1}(M) v^{2m+1}, \quad \forall |v| < V, \quad (5)$$

$$\text{relu}(v) \simeq \frac{v}{2} + \sum_{m=0}^M R_{2m}(M) v^{2m}, \quad \forall |v| < V. \quad (6)$$

In (5) and (6) we require explicit formulas for evaluation to arbitrary precision, yielding expansions valid for a tunable desired bound of validity V . The coefficients are allowed to depend on the order of expansion M . We present the general expansion method which can be applied to a wide class of activations and then apply the method explicitly to $\tanh(v)$, $\text{relu}(v)$, and finally to an entire network layer.

A. General Expansion Technique

The general method for obtaining the coefficients is as follows. First, the function φ to be approximated is expressed via a general Fourier integral transform of the form: $\varphi(v) = \int_{\mathbb{R}} \Phi(\xi) f(\xi v) d\xi$. The kernel $f(\xi v)$ is then expanded via the truncated Taylor series

$$f(\xi v) \simeq \sum_{m=0}^M \tilde{f}(m)(\xi v)^m + \Upsilon_M^{\{f\}}(\xi v), \quad (7)$$

$$\varphi(v) \simeq \int_{\mathbb{R}} \Phi(\xi) \sum_{m=0}^M \tilde{f}(m)(\xi v)^m d\xi. \quad (8)$$

The remainder $\Upsilon_M^{\{f\}}(\xi v)$ is factored into parts $P_M(\xi v)$ and $Q_M(\xi v)$ that increase with and without bound respectively

$$\Upsilon_M^{\{f\}}(\xi v) = P_M(\xi v) Q_M(\xi v). \quad (9)$$

The dominating term $Q_M(\xi v)$ is set equal to a constant C and solved for ξ to determine a suitable limit $\xi = \rho(M)$ of integration for (8) which remains in the region of convergence of (7), i.e., $\xi = Q_M^{-1}(C)/v$. In cases where v varies, the limit of integration can be defined with respect to its maximum V : $\rho_V(M) = Q_M^{-1}(C)/V$. Then Eq. (8) can be rewritten

$$\varphi(v) \simeq \sum_{m=0}^M \tilde{f}(m) v^m \int_{-\rho_V(M)}^{\rho_V(M)} \Phi(\xi) \xi^m d\xi, \quad (10)$$

where the exchange of the summation is permitted since the integral is bounded to the convergent region

$(-\rho_V(M), \rho_V(M))$. Solving the remaining integral yields an approximation in the desired form of (1). By noting the parts of (8) left out by the adjustments an exact expression for the remainder $H_M^{\{\varphi\}}(v)$ is revealed

$$H_M^{\{\varphi\}}(v) = \int_{-\rho_V(M)}^{\rho_V(M)} \Phi(\xi) \Upsilon_M^{\{f\}} d\xi + \int_{-\infty}^{-\rho_V(M)} \Phi(\xi) f(\xi v) d\xi + \int_{\rho_V(M)}^{\infty} \Phi(\xi) f(\xi v) d\xi \quad (11)$$

such that the expansion and its coefficients are given as

$$\varphi(v) \simeq \sum_{m=0}^M \alpha_m(M) v^m \quad \forall |v| < V, \quad (12)$$

$$\alpha_m(M) = \tilde{f}(m) \int_{-\rho_V(M)}^{\rho_V(M)} \Phi(\xi) \xi^m d\xi. \quad (13)$$

B. Alternate Taylor Series Derivation

We derive the Taylor series of $\tanh(v)$ by expressing it in terms of its Fourier transform. Identities from [34] yield

$$\tanh(v) = \lim_{\rho \rightarrow \infty} \int_0^\rho \operatorname{csch}\left(\frac{\pi}{2}\xi\right) \sin(\xi v) d\xi. \quad (14)$$

Expanding the kernel $\sin(\xi v)$ to a partial sum yields

$$\tanh(v) \simeq \lim_{\rho \rightarrow \infty} \sum_{m=1}^M \frac{(-1)^{m-1} v^{2m-1}}{(2m-1)!} \int_0^\rho \xi^{2m-1} \operatorname{csch}\left(\frac{\pi}{2}\xi\right) d\xi. \quad (15)$$

Integrating yields the expansion and exact error, $H_M(v)$:

$$\tanh(v) \simeq \sum_{m=1}^M \frac{2^{2m} (2^{2m} - 1) B_{2m} v^{2m-1}}{(2m)!}, \quad \forall |v| < \frac{\pi}{2}, \quad (16)$$

$$H_M(v) = \frac{(-1)^M v^L}{L!} \int_0^\infty \xi^L \operatorname{csch}\left(\frac{\pi}{2}\xi\right) {}_1F_2(1; b_1, b_2; z) d\xi. \quad (17)$$

Here $L = 2M + 1$, $b_1 = M + 1$, $b_2 = M + 3/2$, and $z = -\frac{v^2 \xi^2}{4}$. Noting that the manipulations of (15) are only valid within the convergent regions of the Taylor expanded kernel $\sin(\xi v)$ illuminates the source of divergence for $|v| \geq \pi/2$ which is then mitigated via the AMITE modifications.

C. Modifying the Limits of Integration

To modify the integral of Eq. (15) so that the resulting expansions are valid for $|v| \geq \frac{\pi}{2}$ we require an upper bound ρ on the domain of validity of the M -term partial sum expanded kernel. Following section III-A we factor the partial sum remainders to consider the dominant factors contributing to divergence. We treat $\sin(\xi v)$ and $\cos(\xi v)$ which are employed subsequently to expand $\tanh(v)$ and $\operatorname{relu}(v)$ as examples illustrating use of the technique on odd and even nonlinearities. We begin with the partial sums

$$\cos(u) = \sum_{m=0}^M \frac{(-1)^m u^{2m}}{(2m)!} + \Upsilon_M^{\{\cos\}}(u), \quad (18)$$

$$\sin(u) = \sum_{m=0}^M \frac{(-1)^m u^{2m+1}}{(2m+1)!} + \Upsilon_M^{\{\sin\}}(u). \quad (19)$$

Factoring the remainders in the form of (9) yields

$$\Upsilon_M^{\{\cos\}}(u) = \frac{(-1)^{M+1} u^{2M+2}}{(2M+2)!} {}_1F_2\left(1; M+2, M+\frac{3}{2}; -\frac{u^2}{4}\right), \quad (20)$$

$$\Upsilon_M^{\{\sin\}}(u) = \frac{(-1)^{M+1} u^{2M+3}}{(2M+3)!} {}_1F_2\left(1; M+2, M+\frac{5}{2}; -\frac{u^2}{4}\right). \quad (21)$$

As u tends to infinity the hypergeometric factors in (20) and (21) tend to zero and the outer factors

$$Q_M^{\{\cos\}}(u) = \frac{u^{2M+2}}{(2M+2)!}, \quad Q_M^{\{\sin\}}(u) = \frac{u^{2M+3}}{(2M+3)!}, \quad (22)$$

tend to infinity. Noting that the outer factors drive the remainders' growth we define the range of validity of the partial sums in (18) and (19) to be all u such that $Q_M^{\{\cos\}}(u) < 1$ and $Q_M^{\{\sin\}}(u) < 1$ respectively. This yields the required bounds on the domain of validity of each partial sum:

$$\cos(u) \simeq \sum_{m=0}^M \frac{(-1)^m u^{2m}}{(2m)!} \quad \forall u < ((2M+2)!)^{\frac{1}{2M+2}}, \quad (23)$$

$$\sin(u) \simeq \sum_{m=0}^M \frac{(-1)^m u^{2m+1}}{(2m+1)!} \quad \forall u < ((2M+3)!)^{\frac{1}{2M+3}}. \quad (24)$$

Noting that the argument to the kernel in (15) is $u = \xi v$, and adjusting for the maximum value $V = \max(v)$, we let σ and τ denote the required upper bounds for integrals in the forms $\int \Phi(\xi) \cos(\xi v) d\xi$ and $\int \Phi(\xi) \sin(\xi v) d\xi$ respectively:

$$\sigma = \frac{((2M+2)!)^{\frac{1}{2M+2}}}{V}, \quad \tau = \frac{((2M+3)!)^{\frac{1}{2M+3}}}{V}. \quad (25)$$

D. Hyperbolic Tangent Expansion

Having identified the bound, τ , for integrals having kernels $\sin(\xi v)$ we can treat the hyperbolic tangent as an exemplary odd nonlinearity. Returning to (15) and integrating the component $\Lambda_j(\xi) = \int \xi^j \operatorname{csch}\left(\frac{\pi}{2}\xi\right) d\xi$ from 0 to τ yields the formulas for the coefficients $T_{2m+1}(M)$ in (5).

$$\tanh(v) \simeq \sum_{m=0}^M T_{2m+1}(M) v^{2m+1} \quad \forall |v| < V, \quad (26)$$

$$T_{2m+1}(M) = \frac{2^{2m+1} (4^{m+1} - 1) B_{2m+2}}{(m+1)(2m+1)!} + \frac{(-1)^{m+1} 4^{2m+1}}{\pi} \sum_{k=0}^{2m+1} \frac{2^k \tau^{2m+1-k} \chi_{k+1}\left(e^{-\frac{\pi\tau}{2}}\right)}{\pi^k (2m+1-k)!}. \quad (27)$$

Here, $\chi_s(z) = \frac{1}{2}(\operatorname{Li}_s(z) - \operatorname{Li}_s(-z))$ denotes Legendre's Chi function. (The result of (27) is derived fully in Appendix A.) The precise remainder follows directly from application of (11):

$$H_M^{\{\tanh\}}(v) = \int_\tau^\infty \operatorname{csch}\left(\frac{\pi}{2}\xi\right) \sin(\xi v) d\xi + \frac{(-1)^{M+1} v^L}{L!} \int_0^\tau \xi^L \operatorname{csch}\left(\frac{\pi}{2}\xi\right) {}_1F_2(1; b_1, b_2; z) d\xi, \quad (28)$$

$$L = 2M + 3, b_1 = M + 2, b_2 = M + \frac{5}{2}, z = -\frac{v^2 \xi^2}{4}. \quad (29)$$

The second term (28) dominates for large v . Since it follows from the Taylor remainder $\Upsilon_M^{\{\sin\}}(\xi v)$ it is small for v within the region of convergence. Meanwhile, the first term in (28) dominates for small v leading to Gibbs-like oscillation of the error for $|v| < V$. Noting this, the first term in (28) can be integrated to analyze errors inside the region of convergence. Let $I_M^{\{\tanh\}}(v)$ denote this error component:

$$\begin{aligned} I_M^{\{\tanh\}}(v) &= \int_{\tau}^{\infty} \operatorname{csch}\left(\frac{\pi}{2}\xi\right) \sin(\xi v) d\xi \\ &= 2 \tanh(v) - \frac{i}{\pi} (\operatorname{B}_{e^{\pi\tau}}(a, 0) - \operatorname{B}_{e^{\pi\tau}}(a^*, 0)), \end{aligned} \quad (30)$$

Here, $\operatorname{B}_z(a, b)$ denotes the Incomplete Beta function and $a = \frac{1}{2} + \frac{iv}{\pi}$. Rearranging (30) to extract the dominant oscillating factor, noting that for $a = \frac{1}{2} \pm \frac{iv}{\pi}$

$$\operatorname{B}_{e^{\pi\tau}}(a, 0) = \frac{e^{\frac{\pi\tau}{2}} e^{\pm i\tau v}}{a} {}_2F_1\left(1, a; \frac{3}{2} \pm \frac{iv}{\pi}; e^{\pi\tau}\right), \quad (31)$$

and substituting this result (31) into (30) reveals

$$I_M^{\{\tanh\}}(v) = \frac{e^{\frac{\pi\tau}{2}}}{e^{\pi\tau} - 1} (UF + U^*F^*), \quad (32)$$

$$U = \frac{e^{-i\tau\pi}}{v - \frac{i\pi}{2}}, \quad F = {}_2F_1\left(1, 1; \frac{3}{2} + \frac{iv}{\pi}; \frac{1}{1 - e^{\pi\tau}}\right). \quad (33)$$

Recalling from (25) that τ increases with the number of terms M and noting $\lim_{\tau \rightarrow \infty} {}_2F_1\left(1, 1; c; \frac{1}{1 - e^{\pi\tau}}\right) = 1$ reveals a remarkably accurate approximate closed form for the error within the convergent region $|v| < V$:

$$I_M^{\{\tanh\}}(v) \simeq \frac{4e^{\frac{\pi\tau}{2}} (\pi \sin(\tau v) + 2v \cos(\tau v))}{(e^{\pi\tau} - 1)(4v^2 + \pi^2)} \quad (34)$$

From (34) we can deduce that within the convergent region the error will oscillate with approximate period of $\frac{2\pi}{\tau}$ and amplitude dependent on v and τ . Since τ increases with respect to M and $\lim_{\tau \rightarrow \infty} e^{\frac{\pi\tau}{2}} (e^{\pi\tau} - 1)^{-1} = 0$ we deduce from the exact expression (32) for $I_M^{\{\tanh\}}(v)$ that $\lim_{M \rightarrow \infty} I_M^{\{\tanh\}}(v) = 0$ as is required to achieve a low error within $(-V, V)$.

E. An Improved ReLU Expansion

Here we expand $\operatorname{relu}(v)$, again following Section III-A. Since the odd part, v , of $\operatorname{relu}(v)$ is trivial, we begin by expressing the even part in terms of its Fourier transform

$$|v| = -\frac{1}{\pi} \lim_{\rho \rightarrow \infty} \int_{-\rho}^{\rho} \frac{\cos(\xi v)}{\xi^2} d\xi. \quad (35)$$

We then apply our bound σ for integrals involving $\cos(v\xi)$ as per (25) so that we may expand the kernel as a partial sum and exchange the order of summation as per (10) yielding

$$|v| \simeq -\frac{1}{\pi} \sum_{m=0}^M \frac{(-1)^m v^{2m}}{(2m)!} \int_{-\sigma}^{\sigma} \xi^{2m-2} d\xi. \quad (36)$$

Solving directly and adding back in the odd part of $\operatorname{relu}(v)$ yields the desired formulas in Eq. (6).

$$\operatorname{relu}(v) \simeq \frac{v}{2} + \sum_{m=0}^M R_{2m}(M) v^{2m} \quad \forall |v| < V, \quad (37)$$

$$R_{2m}(M) = \frac{(-1)^{m+1} \sigma^{2m-1}}{\pi (2m)! (2m-1)}. \quad (38)$$

Again, the precise remainder follows from (11):

$$H_M^{\{\operatorname{relu}\}}(v) = -\frac{1}{\pi} \int_{\sigma}^{\infty} \frac{\cos(\xi v)}{\xi^2} d\xi \quad (39)$$

$$+ \frac{(-1)^M v^{2M+2}}{\pi (2M+2)!} \int_0^{\sigma} \xi^{2M} {}_1F_2(1; b_1, b_2; z) d\xi,$$

$$b_1 = M+2, b_2 = M + \frac{3}{2}, z = -\frac{v^2 \xi^2}{4}. \quad (40)$$

The integrals can be readily solved yielding

$$\begin{aligned} H_M^{\{\operatorname{relu}\}}(v) &= \frac{|v|}{2} - \frac{v \operatorname{Si}(\sigma v)}{\pi} - \frac{\cos(\sigma v)}{\sigma} \\ &+ \frac{(-1)^M \sigma^{2M+1} v^{2M+1}}{\pi (2M+2)(2M+1)!} {}_2F_3(1, a; b, b, c; z), \end{aligned} \quad (41)$$

$$a = M + \frac{1}{2}, b = M + \frac{3}{2}, c = M + 2, z = -\frac{\sigma^2 v^2}{4}. \quad (42)$$

Due to the v^{2M+1} factor, the second term of (41) dominates outside the region of convergence. Meanwhile, the first term dominates for small v leading to Gibbs-like oscillation within the region of convergence $|v| < V$. The exact expression for the oscillating component of the error, $I_M^{\{\operatorname{relu}\}}(v)$, is given by

$$I_M^{\{\operatorname{relu}\}}(v) = \frac{|v|}{2} - \frac{v \operatorname{Si}(\sigma v)}{\pi} - \frac{\cos(\sigma v)}{\sigma}. \quad (43)$$

As with $\tanh(v)$, since σ increases with respect to the number of terms, M , and then since $\lim_{\sigma \rightarrow \infty} I_M^{\{\operatorname{relu}\}}(v) = 0$ we can again deduce that $\lim_{M \rightarrow \infty} I_M^{\{\operatorname{relu}\}}(v) = 0$ as is required to achieve low error within the convergent region.

F. Full Layer Expansion

The coefficients, α_j , of the activations, φ , can then be used to expand a full network layer as a polynomial. To perform this expansion, we substitute the hidden neuron input as defined in Eq. (3) into Eq. (1).

$$\varphi(v_n) \simeq \sum_m \alpha_j \left(b_n^{\{0\}} + \sum_{i=1}^{N_I} w_{n,i}^{\{0\}} x_i \right)^j, \quad (44)$$

Here j is the exponent belonging to each index m . Applying the multinomial expansion gives

$$\varphi(v_n) \simeq \sum_m \sum_{|\kappa|=j} \alpha_j \binom{j}{\kappa} \vartheta_n^{\kappa} x^{\kappa}, \quad (45)$$

$$\vartheta_n = \left(b_n^{\{0\}} \quad w_{n,1}^{\{0\}} \quad \cdots \quad w_{n,N_I}^{\{0\}} \right). \quad (46)$$

Here $\kappa = [\kappa_1, \kappa_2, \dots, \kappa_{N_I+1}]$ is a multi-index where $u^{\kappa} = \prod_i u_i^{\kappa_i}$, $|\kappa| = \sum_i \kappa_i$, and $\binom{j}{\kappa} = \frac{j!}{\kappa_1! \kappa_2! \cdots \kappa_N!}$ is a multinomial coefficient. The output of the layer can then be approximated by taking the weighted sum of the neuron outputs:

$$y(\alpha, \beta, x) \simeq b^{\{1\}} + \sum_{n=1}^{N_H} \sum_m \sum_{|\kappa|=j} \alpha_j(M) \binom{j}{\kappa} w_n^{\{1\}} \vartheta_n^{\kappa} x^{\kappa} \quad (47)$$

We use $\Psi_{\kappa}(\alpha, \beta)$ to denote the coefficient associated with the term $x^{\kappa} = x_1^{\kappa_1} x_2^{\kappa_2} \cdots x_{N_I+1}^{\kappa_{N_I+1}}$ in the polynomial approximation of $y(\alpha, \beta, x)$. By definition of $\Psi_{\kappa}(\alpha, \beta)$ we can write:

$$y(\alpha, \beta, x) \simeq \sum_{\kappa} \Psi_{\kappa}(\alpha, \beta) x^{\kappa} \quad (48)$$

IV. EXPANSION RESULTS

To verify the analysis of Section III we evaluate the expansions for tanh and relu. In each evaluation, we first compare the approximation values $\varphi_a(v) \simeq \sum_{m=0}^M \alpha_m v^m$ to the true function values $\varphi(v)$ over v in $(-V - c, V + c)$ where c is small value chosen to show performance just outside of the domain of validity $(-V, V)$. We then show the measured error $E_M^{\{\varphi\}}(v) = \varphi(v) - \varphi_a(v)$, exact error $H_M^{\{\varphi\}}(v)$, and analytic approximate error $I_M^{\{\varphi\}}(v)$. Finally, we display the errors between the error formulas themselves and the measured errors, $|E_M^{\{\varphi\}}(v) - H_M^{\{\varphi\}}(v)|$ and $|E_M^{\{\varphi\}}(v) - I_M^{\{\varphi\}}(v)|$.

Expansions and errors are shown in Fig. 1 and Fig. 2. Formulas to compute coefficients are evaluated in 450 digits of precision and the polynomials themselves are evaluated in IEEE 754 double precision floating point arithmetic. Satisfaction of the qualitative properties described in Table I is summarized in Table II. We find that the *exact coeffs.*, *monic form*, *adjustable domain*, and *handles undef. derivs.* properties are satisfied by (26) and (37). The *explicit exact errors* property is satisfied by (28) and (28) and (41). The *consistent method* property is satisfied by Section III-A.

V. CASE STUDY: APPLYING AMITE TO MLP EQUIVALENCE TESTING

A. Definitions

In this case study, we employ the following definitions. An *original network* is a neural network, created by a designer, e.g., in software. A *network under test* is an implemented neural network (e.g., in hardware) which a test procedure must determine to be output-equivalent to the original network. The *stimulus signal* is the signal applied and the *response signal* is the output signal measured, including measurement noise. A *replicated network* is defined as the network having weights extracted from the network under test. A network under test is confirmed to be *output-equivalent* to the original network if it is shown that they will produce sufficiently close outputs for all inputs in a given interval, according to a provided error metric.

B. Experimental Setup

The experimental process was modeled computationally on a Dell XPS Laptop running Python 3.7, using the pytorch, numpy, cupy, and mpmath libraries, on an Nvidia GeForce GTX 1650 GPU with 1024 Cuda Cores and an Intel i9-9980HK CPU at 2.40GHz. Parallel processing was implemented through pytorch and cupy matrix operations. Coefficients for tanh and relu were precomputed using 450 digits of precision via the precise formulas of Section III and polynomials were evaluated at runtime in IEEE 754 double precision floating point arithmetic. Mathematical primitives including binomial and multinomial coefficients were pre-computed and stored in hashmaps. Multinomial coefficient hashmaps required 4.73GB of disk space and were loaded into program memory as needed in chunks ranging from 11KB to 986MB for fast access.

Hyperbolic Tangent Expansion for $M = 25, V = 20$

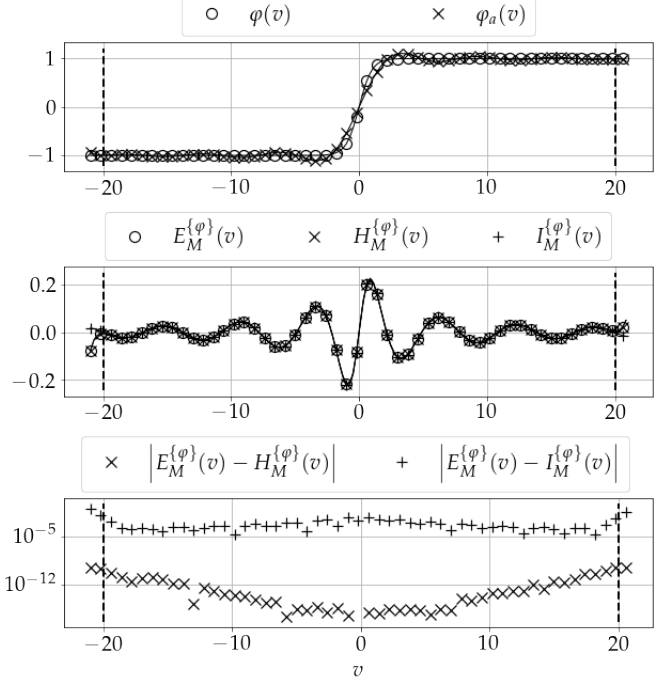


Fig. 1. Expansion results and errors for $\varphi(v) = \tanh(v)$, number of terms $M = 25$ and validity parameter $V = 20$. Top: expansion $\varphi_a(v)$ and true function $\varphi(v)$; middle: measured error $E_M^{\{\varphi\}}(v)$, exact error $H_M^{\{\varphi\}}(v)$, approximate error $I_M^{\{\varphi\}}(v)$; bottom: difference between measured errors and predicted errors.

ReLU Expansion for $M = 25, V = 20$

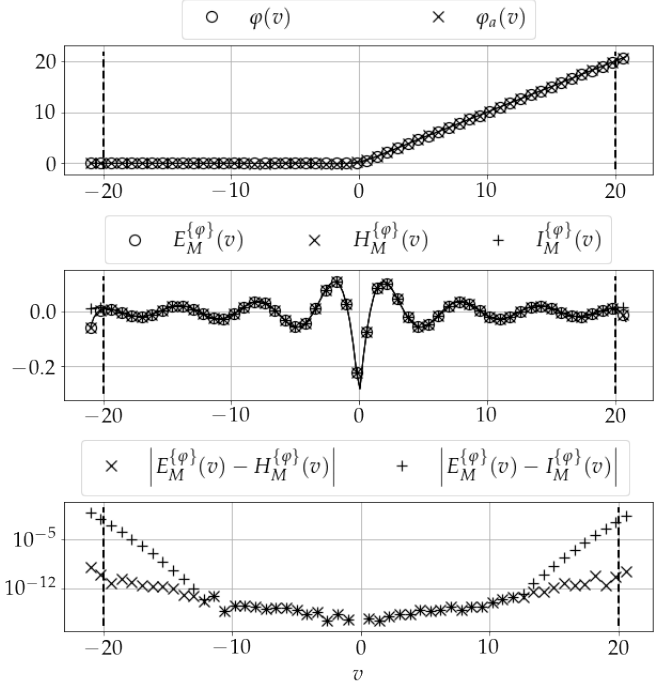


Fig. 2. Expansion results and errors for $\varphi(v) = \text{relu}(v)$, number of terms $M = 25$ and validity parameter $V = 20$. Top: expansion $\varphi_a(v)$ and true function $\varphi(v)$; middle: measured error $E_M^{\{\varphi\}}(v)$, exact error $H_M^{\{\varphi\}}(v)$, approximate error $I_M^{\{\varphi\}}(v)$; bottom: difference between measured errors and predicted errors.

C. Example Application to Equivalence Testing

As a first example, we consider a single hidden layer MLP used to control a fielded hardware system. In such applications, it can be advantageous to rapidly develop models via open-source software [35]–[37] and then exploit the efficiency of numerous proposed hardware approaches for implementation [38]–[41]. However, separating design from implementation motivates the question: how does one confirm that the network implemented in hardware is output-equivalent to the network designed? The answer is complicated by equivalent configurations of a given network [42], [43] and by small parameter perturbations yielding approximately equivalent input-output pairs [44]. Measurement noise obscures the true error between the implemented input-output map and the original input-output map and due to nonlinearity, it is unclear what degree of deviation represents a defect.

To show how AMITE can be applied here, we develop a bug-finding “conformance test” to address the challenges above. First, we extract the weights of the implemented network following the methods of model stealing / replication [45]–[49] to fit a new model to a set of stimulus-response pairs. Then following the methods of Section III we analytically convert the weights of a single network layer to an AMITE polynomial and compare the coefficients to the AMITE representation of the original network. Here the AMITE coefficients provide a means to assess equivalence directly from the replicated and original weights.

The preceding replication step is used to provide a guarantee that the stimulus applied yields suitable coverage to achieve a comprehensive equivalency test. If the test signal does not provide sufficient coverage invalid weights will be extracted and the test will fail. This step biases the test towards a low false negative rate while offering the opportunity to further inspect a failed result by adding more test inputs. The observed efficacy of the equivalency test is dependent on the expansion technique’s ability to accurately and efficiently expand an entire network layer as a polynomial over a desired domain. This first case study assumes low dimensional, normalized inputs and assumes the expected structure of the network under test is known while its actual structure is unknown.

D. MLP Equivalence Test Steps

The specific steps of the equivalency test used are as follows. First, an interrogation signal, $x_I(t)$, consisting of white noise fuzz vectors is activated to stimulate the implemented network. Measured output with any incurred noise \mathcal{N} is collected and denoted $\hat{y}_I(t) = y(\alpha, \beta_I, x_I(t)) + \mathcal{N}$. The input-output pairs (x_I, y_M) are then used to solve for the replicated network weights β_R by fitting:

$$\beta_R = \arg \min_{\beta} \left((\hat{y}_I(t) - y(\alpha, \beta, x_I(t)))^2 \right) \quad (49)$$

Since the expected β values are known in advance, they are used as a starting point for fitting to expedite extraction of β_R and avoid false positives due to multiple local minima. The optimization problem is solved over 250 fuzz vectors x_I via stochastic gradient descent with adaptive learning

Example Bug Detection Test

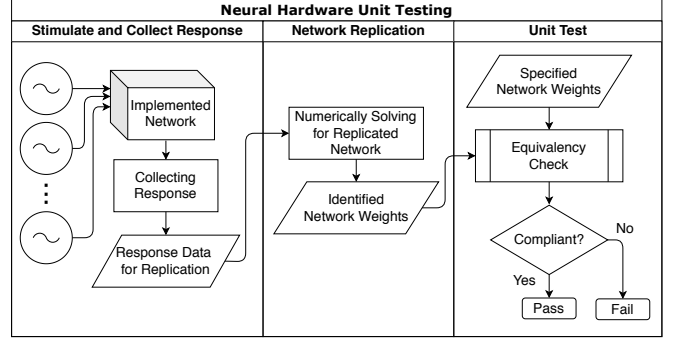


Fig. 3. Unit level bug-finding conformance test procedure applying network replication to test an implemented MLP for equivalence to an original MLP. An implemented network of known expected structure with unknown weights and unknown structure is stimulated by a plurality of signals and the unknown weights are identified from the response. The identified weights are converted to AMITE representations and checked for equivalency to the specified weights to determine if the networks match.

rate starting at $l = 1 \times 10^{-3}$, weight decay $d = 0.01$, and no momentum. The original and replicated networks are then represented analytically via the methods of Section III-F as multivariate AMITE polynomials having coefficients $\Psi(\alpha, \beta_O) = [\Psi_{r_n}(\alpha, \beta_O)]$ and $\Psi(\alpha, \beta_R) = [\Psi_{r_n}(\alpha, \beta_R)]$ respectively. To check equivalency, we use a mean absolute logarithmic error between the magnitudes of the coefficients:

$$\eta(\Psi(\alpha, \beta_R), \Psi(\alpha, \beta_O)) = \text{mean} |\log(\epsilon + |\Psi(\alpha, \beta_O)|) - \log(\epsilon + |\Psi(\alpha, \beta_R)|)|. \quad (50)$$

If the error η is below a set threshold ϵ the networks are determined to be equivalent. These steps are summarized in Fig. 3.

E. Network Equivalency Testing Results

To collect results for the method of section V-D, a population of 90 MLPs is instantiated having inputs $N_I \in \{1, 2, 3\}$ and number of hidden nodes $N_H \in \{5, 10, 35, 75, 125\}$. The population is duplicated to model a set of networks under test. Defects in the form of random weight perturbations are introduced into half of the population of networks under test. The network equivalency test of Fig. 3 is executed following the methods of Section V-D on each network. All 90 networks are tested with varying noise $\mathcal{N} \in \{-20, -10, -1, 0, 1, 10, 20\}$. The entire procedure is repeated three times for a total of 1890 calls to the test. The accuracy at finding bugs is reported in Fig. 4 with respect to signal to noise ratio in the measured outputs. The runtimes with respect to number of hidden nodes and number of inputs are reported in Fig. 5 and 6. For all tests an error threshold of $\epsilon = 0.01$ was applied when checking equivalency by the metric of (50): $\eta(\Psi(\alpha, \beta_R), \Psi(\alpha, \beta_O)) > \epsilon$. We find that the test completes in under 7 seconds on average for low-dimensional input (2-4 inputs) MLPs having up to 125 hidden nodes. The runtime per test is inclusive of both solving for the replicated network parameters and computing the AMITE polynomial representation.

Bug Detection Accuracy wrt. Measurement Noise

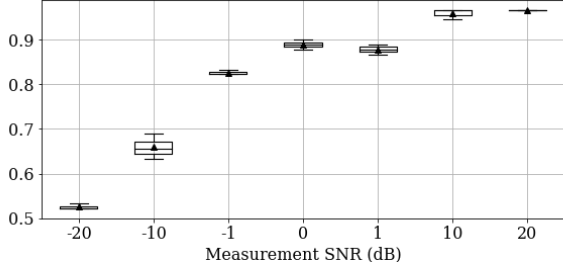


Fig. 4. Bug detection accuracy with respect to measurement noise. The fraction of defective networks under test which were correctly identified is shown here with respect to measurement noise. Results are aggregated over 1890 calls to the equivalency test on networks of varying sizes under various levels of noise.

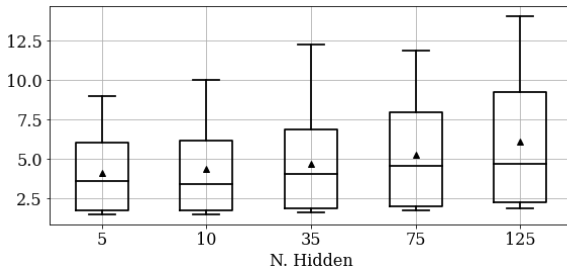
Runtime (s) wrt. Number of Hidden Units, (N_H)

Fig. 5. Runtime per call to the test with respect to number of hidden units, N_H . Statistics are computed across 1890 calls to the test.

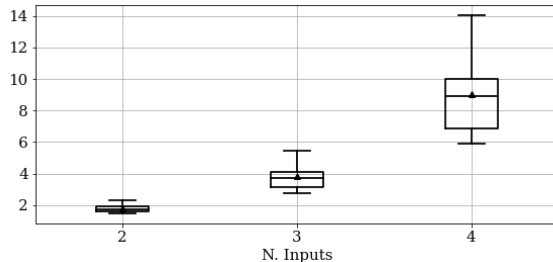
Runtime (s) wrt. Number of Inputs, (N_I)

Fig. 6. Runtime per call to the test with respect to number of inputs, N_I . Statistics are computed across 1890 calls to the test.

VI. CASE STUDY: RANGE BOUNDING DEEP FFNNs VIA AMITE BASED TAYLOR MODELING

A. Experimental Setup

The experimental setup is identical to the previous case study except for the digits of precision (DP) used to compute the coefficients, which are reduced to 65 for the smaller networks and increased up to 450 as needed. A custom Taylor modeling library was implemented in Python 3.7 allowing traditional Taylor series or AMITE polynomials to be used in constructing Taylor models for comparison. A subset of IEEE 1788.1 interval arithmetic was implemented for handling error intervals.

B. Example Application to Range Bounding Deep FFNNs

This application is identical in setup and motivation to the previous application, except that we now desire formal bounds on the outputs of a neural network which will control a fielded hardware system. For example, if the network is providing acceleration commands, it may be required to confirm that the acceleration commands will never exceed certain values as long as the input remains in a restricted domain. The range analysis problem has been studied in depth in the neural network literature and for nonlinear systems in general. A well-known tool for performing this analysis is Taylor models [31], [32], however it is also known [2], [50] that straightforward application of Taylor models to deep FFNNs leads to over-approximation of errors.

In this example application, we address the problem of over-estimation of errors analytically, employing the formulas of Section III to inform the generation of Taylor models for the networks under test, allowing efficient generation of tighter range bounds for deep FFNNs over larger domain intervals than possible with an unmodified Taylor model. Use of such methods in critical applications, such as [7], further motivates the use of analytic methods in complement to the existing repertoire of numerical methods for improving Taylor models.

C. Improved Taylor Modeling and Range Bounding Procedure

The improved Taylor modeling and range bounding procedure for neural networks enabled by the AMITE polynomials is described as follows. First, the weights of the network and the desired domain intervals $x_n \in \mathcal{I}_n$, $\mathcal{I}_n = (x_{n,\min}, x_{n,\max})$ for each input x_n of the network are provided as procedure inputs. The network to be range bounded is then stimulated via random white-noise fuzz vectors in \mathcal{I}_n to obtain a suitable initial guess for the required domain of validity V . A conservative value $V = S \max(v)$ is chosen where S is a safety factor. AMITE polynomials are computed for the activation function given the detected V and a desired number of terms M . The AMITE polynomials are then used as the coefficients $[\alpha_m]$ in the Taylor model.

To efficiently determine the error bounds on the Taylor model, the minimum and maximum error between the polynomial determined by $[\alpha_m]$ and the true activation function φ over \mathcal{I}_n must be determined. To do this efficiently, we first exploit the accurate simplified error approximations, $I_M^{\{\varphi\}}(v)$, derived in Section III. Since these formulas are efficient to compute, a course grid search over their range on the given domain is performed to identify an initial estimate for the locations of the maximum and minimum errors. These locations and the known periods of oscillation in the errors, also derived in Section III, are employed to identify a bounded optimization region within one half period in either direction of the initial estimate.

A bounded optimizer is then employed to optimize over the exact error formula, $H_M^{\{\varphi\}}(v)$, and find the precise maximum and minimum errors within a defined optimizer tolerance. The optimizer tolerance is then added via interval addition to the error interval to obtain a formal error bound on the expansion to be used in the Taylor model as (e_{\min}, e_{\max}) . As such,

Results for Range Bounding Deep FFNNs via Taylor Models Enhanced with AMITE Polynomials

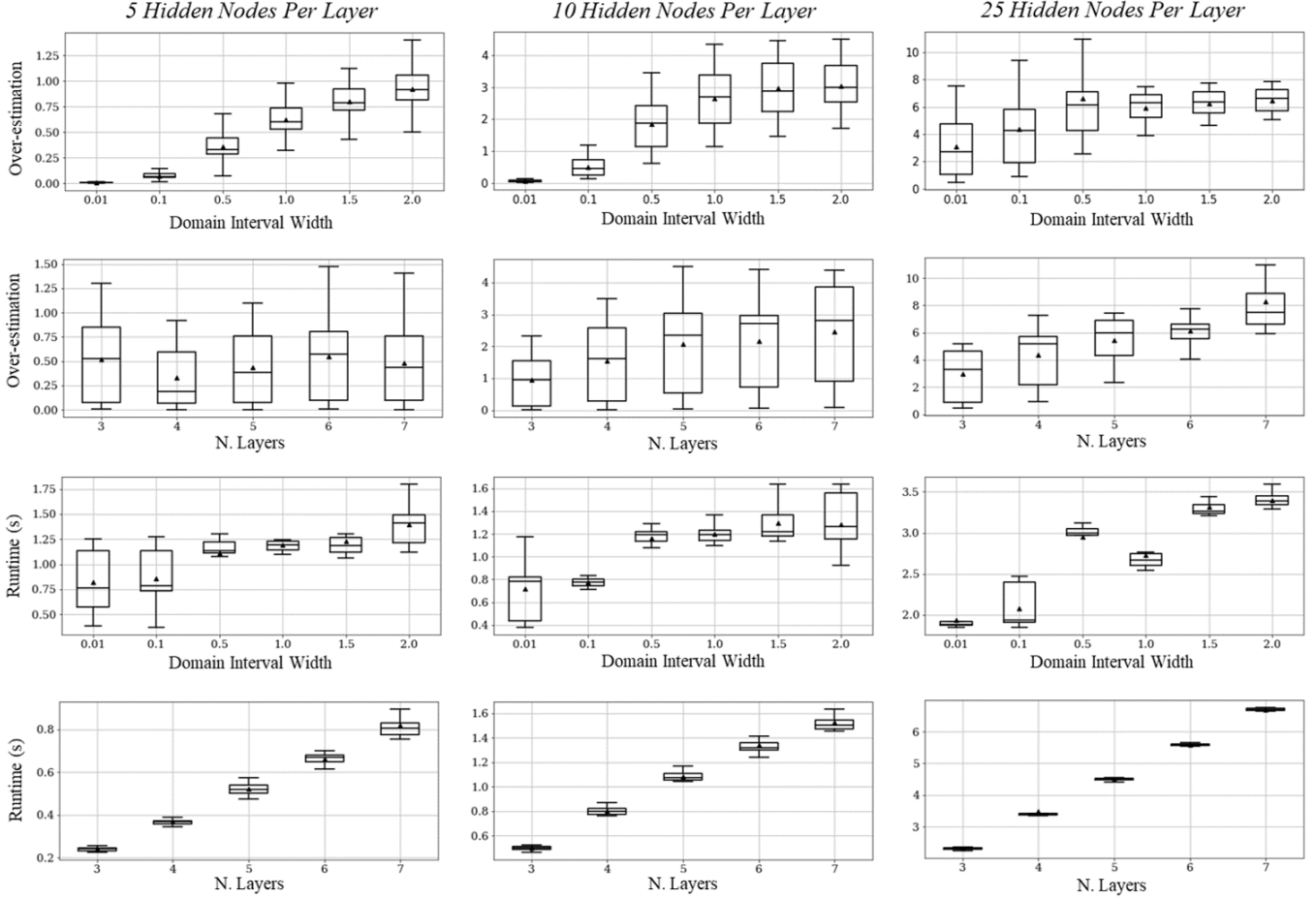


Fig. 7. Range bounding results over a population of deep FFNNs. Here each network in a population of deep FFNNs (3-7 layers and 5-25 hidden neurons per layer) is range bounded numerically via random stimulation and rigorously via Taylor models employing AMITE polynomials. In the top row, over-estimation of the Taylor models compared to the numerical estimate is shown. In the second row, over-estimation is shown with respect to the number of hidden layers. In the third row, the runtime required to generate the AMITE polynomials (one time cost) is shown with respect to the interval width the polynomials were optimized for. In the bottom row, the runtime to range bound each network is shown with respect to the number of hidden layers.

a formal error bound is given with a minimum number of expensive calls to evaluate the exact error function. With a Taylor model, $\mathcal{T} = ([\alpha_m], (e_{\min}, e_{\max}))$, obtained for $\varphi(v)$, the rules of Taylor model and interval arithmetic are then used to propagate the input domains \mathcal{I}_n through the network, adjusting the error interval after each operation. If at any time divergence is encountered (e.g., due to infinite results), the procedure returns to the first step and increases the safety factor S before the Taylor model is reconstructed over a wider domain and the subsequent steps are repeated.

D. Range Bounding Results

To collect results for range bounding example, a population of 60 deep FFNNs is instantiated having 3 inputs, a uniform number of hidden nodes per layer $N_H \in \{5, 10, 25\}$, and layers $N_L \in \{3, 4, 5, 6, 7\}$. The range bounding procedure is then run on each network to analyze several input interval widths. For $N_H = 5, 10$, $M = 6$ is used with 65 DP. For $N_H = 25$, $M = 12$ is used with 130 DP. For $N_H = 50$, $M = 25$ is used with 260 DP. Each network is range

bounded for input intervals centered about zero having widths $W \in \{0.01, 0.1, 0.5, 1, 1.5, 2.0\}$. Evaluating 15 networks over 6 intervals per network yields 90 calls to the test procedure per network architecture for a total of 360 calls to the procedure. Each input is set to the same domain interval for simplicity. For each network, its range bounds are first estimated numerically by stimulating the network with 100 random inputs inside the domain interval. Then the range bounds are estimated via a traditional Taylor model and via a Taylor model constructed from AMITE polynomials.

For each network, the range overestimation via traditional Taylor models, range overestimation via AMITE improved Taylor models, runtime to generate the AMITE coefficients, and runtime to execute the range bounding procedure are tabulated. The range overestimation is defined to be the width of the Taylor model interval minus the width of the interval found by taking the maximum and minimum outputs resulting from random stimulation. Since the true range is unknown in all cases, we note that the numerical estimate likely underestimates the true range since random stimulation

Results for Range Bounding Deep FFNNs via Traditional Taylor Models with Taylor Series

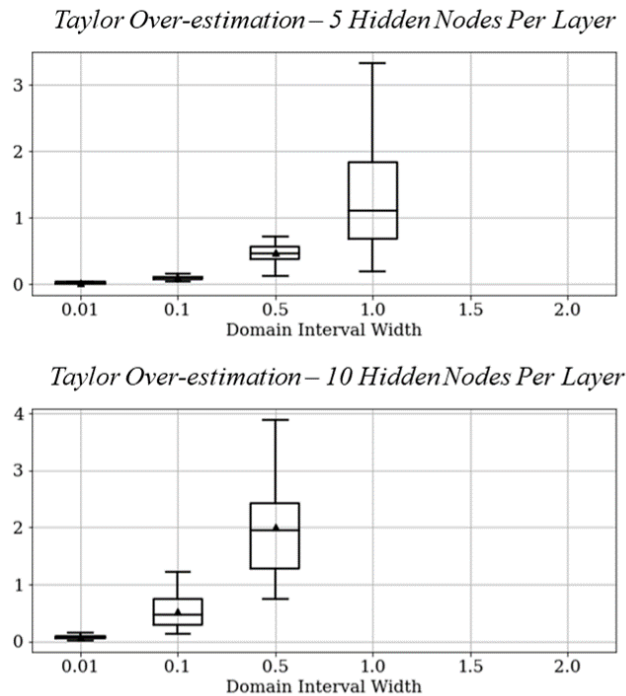


Fig. 8. Range bounding results over a population of deep FFNNs via traditional Taylor models with Taylor Series. Range bounds over a population of deep FFNNs are shown as computed via conventional Taylor models for domain input intervals of increasing width. The rapid expansion of the range interval overestimation with respect to the input interval width is shown. Note that the conventional Taylor model diverges for inputs greater than $\frac{\pi}{2}$. Propagation of errors through the network can cause the model to diverge sooner.

is not guaranteed to excite steep nonlinearities in the network’s input-output manifold. Since `relu` does not have a conventional Taylor series, a `tanh` activation function is used throughout to enable direct comparison between conventional Taylor models (via Taylor series) and Taylor models constructed from AMITE polynomials. We note that conventional Taylor models diverged to infinity for many cases tested. While this could be resolved by subdividing the domain into smaller intervals a single interval was employed in all cases for a one-to-one comparison.

Results for using AMITE polynomials to construct Taylor models to range bound deep FFNNs and overestimation compared to numerically estimated bounds are shown in Fig. 7. Results using conventional Taylor modeling to attempt the same range bounding on network architectures where this is feasible are shown in Fig. 8. In a final experiment to demonstrate a practical application, a set of 4 wide networks of similar architecture (1 hidden layer, 12K hidden nodes, `relu` activation) to those which Pope et al. trained to defeat human pilots in simulated F-16 air-to-air combat [7] is range bounded over increasingly wide input intervals using AMITE polynomials. Results for this experiment are shown in Fig. 9. Runtime to perform the range bounding was averaged 264 seconds per network. Runtime to generate the AMITE

Results for Range Bounding Wide MLPs via Taylor Models Enhanced with AMITE Polynomials

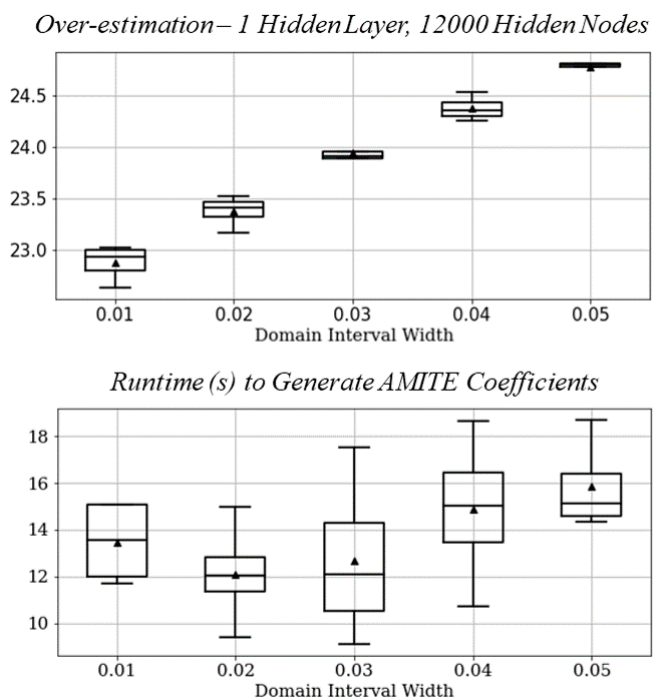


Fig. 9. Range bounding results for wide MLPs via Taylor models enhanced with AMITE polynomials. Here range bounds for 4 MLPs, each having 1 hidden layer and 12000 hidden nodes are computed using AMITE enhanced Taylor models for several domain interval widths and shown in the top plot. Runtime (s) to generate the AMITE polynomial coefficients is shown in the bottom plot with respect to the domain interval width the coefficients were generated for.

coefficients optimized for each interval size is between 9 and 19 seconds. We note that due to the size of the network and use of `ReLU`, a conventional Taylor model could not be employed.

VII. RELATED WORK

This work is intended to apply to several sub-fields of research in neural networks, and is particularly related to neural systems verification, equivalency testing, and to model replication attacks. Recent work on neural network verification focus on defense against and identification of adversarial perturbations [51], [52], output reachable set estimation [53], and computing upper bounds on error rates under adversarial attack [54]. Liu et al. survey algorithms for verifying deep neural networks and categorize them into forms of reachability analysis, optimization to falsify an assertion, and search to falsify an assertion [55]. Bunel et al. present a unifying framework for the formal verification of piecewise linear neural networks [56].

Other significant studies present output range analysis via over-approximation [57] [58] and via exact (sound and complete) methods [59] [60], verification against a specification [61], and a hybrid systems approach to verifying properties of neural network controllers with sigmoid activations [62]. A survey of the safety and trustworthiness of deep neural networks is provided by Huang et al. [63]. A review of the

state of the art in testing AI systems for safety and robustness is provided by Wu et al. [64].

Methods of identifying equivalent neural networks given a matrix of neuron outputs are available [65]–[68] and have recently been advanced by Kornblith et al. [69]. Methods to identify opportunities for compressing a neural network [70], [71] and for perturbing parameters to identify output-equivalent neural networks are also available [44].

VIII. CONCLUSION

In this paper we have developed a novel polynomial expansion technique, the analytically modified integral transform expansion (AMITE), to enable for the first time decomposing neural network activation functions into polynomial forms having six advantageous properties, including exact formulas, monic form, adjustable domain, and robustness to undefined derivatives. To complement the exact formulas, convenient closed-form approximations of the exact expansion errors have been developed by exploiting relationships amongst the special functions arising therein. We have demonstrated the effectiveness of AMITE in two case studies. First, a method for decomposing a single hidden layer into an multivariate polynomial is derived and applied to an illustrative MLP equivalence testing problem where a black-box network under test is stimulated, and a replicated multivariate polynomial form is efficiently extracted from a noisy response to enable comparison against an original network. We then demonstrate the effectiveness of AMITE for generating improved Taylor models for deep FFNNs which allow efficiently obtaining tighter range bounds over larger input intervals than possible via conventional Taylor models. Our future work focuses on combining both case studies to efficiently extract Taylor models of black box deep FFNNs from noisy stimulus-response pairs, thus allowing range bounding of neural networks for which the user has no access to the internal parameters.

APPENDIX A

Here we present a full derivation of the result of eq. (27) in section III. This equation gives the formula for the coefficients of the improved $\tanh(v)$ expansion and follows from the integral $\int \xi^j \operatorname{csch}(\frac{\pi}{2}\xi) d\xi$. We solve this integral by starting with a trivially more general one, $\int \xi^j \operatorname{sech}(a\xi + b) d\xi$, and exploiting the basic relation $\operatorname{sech}(a\xi + \frac{i\pi}{2}) = -i \operatorname{csch}(a\xi)$, between the hyperbolic functions such that the result may be readily applied to a class of related functions. Starting with repeated integration by parts

$$\begin{aligned} & \int \xi^j \operatorname{sech}(a\xi + b) d\xi = \\ & (-1)^j \int \frac{\partial^j}{\partial \xi^j} \xi^j \left(\underbrace{\int d\xi \cdots \int d\xi}_{j} \operatorname{sech}(a\xi + b) \right) d\xi \\ & + \sum_{k=0}^{j-1} (-1)^k \frac{\partial^k}{\partial \xi^k} \xi^j \frac{\partial^{j-k-1}}{\partial \xi^{j-k-1}} \underbrace{\int d\xi \cdots \int d\xi}_{j} \operatorname{sech}(a\xi + b). \end{aligned} \quad (51)$$

Repeated differentiation of the hyperbolic is presented in full generality by [72]. Here we employ a simpler formula for repeated integration revealed by expressing $\operatorname{sech}(a\xi + b)$ in terms of the polylogarithms:

$$\begin{aligned} & \underbrace{\int d\xi \cdots \int d\xi}_{j} \operatorname{sech}(a\xi + b) = \\ & \frac{i(-1)^j}{a^j} \left(\operatorname{Li}_j(-ie^{-a\xi+b}) - \operatorname{Li}_j(ie^{-a\xi-b}) \right). \end{aligned} \quad (52)$$

Applying to (51) yields the useful intermediate result

$$\int \xi^j \operatorname{sech}(a\xi + b) d\xi = -\frac{2}{a} \sum_{k=0}^j \frac{j! \xi^{j-k} \operatorname{Ti}_{k+1}(e^{-a\xi-b})}{a^k (j-k)!}. \quad (53)$$

Here $\operatorname{Ti}_s(z)$ denotes the Inverse Tangent Integral, defined by $\operatorname{Ti}_s(z) = \frac{1}{2i} (\operatorname{Li}_s(iz) - \operatorname{Li}_s(-iz))$. Noting the relationship $i\operatorname{Ti}_s(-iz) = \chi_s(z)$ and the relationship between $\operatorname{csch}(z)$ and $\operatorname{sech}(z)$ reveals

$$\begin{aligned} \Lambda_j(\xi) &= \int \xi^j \operatorname{csch}(a\xi) d\xi \\ &= -\frac{2}{a} \sum_{k=0}^j \frac{j! \xi^{j-k} \chi_{k+1}(e^{-a\xi})}{a^k (j-k)!}. \end{aligned} \quad (54)$$

The expression for the coefficient $T_{2m+1}(M)$ in (5) then follows directly from (13). The integral is evaluated to the bound τ corresponding to the kernel $\sin(\xi v)$ such that

$$\begin{aligned} T_{2m+1} &= \frac{(-1)^m}{(2m+1)!} \int_0^\tau \xi^{2m+1} \operatorname{csch}\left(\frac{\pi}{2}\xi\right) d\xi \\ &= \frac{(-1)^m}{(2m+1)!} \left(\Lambda_{2m+1}(\tau) - \lim_{\varepsilon \rightarrow 0} \Lambda_{2m+1}(\varepsilon) \right). \end{aligned} \quad (55)$$

Noting that

$$\frac{1}{2} \lim_{\xi \rightarrow 0} \xi^{j-k} \operatorname{Li}_{k+1}\left(e^{-\frac{\pi\xi}{2}}\right) = \begin{cases} \frac{1}{2} \zeta(k+1) & j = k \\ 0 & j \neq k, \end{cases} \quad (57)$$

$$\begin{aligned} & \frac{1}{2} \lim_{\xi \rightarrow 0} \xi^{j-k} \operatorname{Li}_{k+1}\left(-e^{-\frac{\pi\xi}{2}}\right) \\ &= \begin{cases} \frac{1}{2} (2^{-k} - 1) \zeta(k+1) & j = k \\ 0 & j \neq k, \end{cases} \end{aligned} \quad (58)$$

and the relation, $\zeta(2m) = (-1)^{m+1} (2\pi)^{2m} B_{2m} (2(2m)!)^{-1}$, between the Riemann Zeta function and the Bernoulli numbers yields the result of (27):

$$\begin{aligned} T_{2m+1}(M) &= \frac{2^{2m+1} (4^{m+1} - 1) B_{2m+2}}{(m+1)(2m+1)!} \\ &+ \frac{(-1)^{m+1} 4}{\pi} \sum_{k=0}^{2m+1} \frac{2^k \tau^{2m+1-k} \chi_{k+1}(e^{-\frac{\pi\tau}{2}})}{\pi^k (2m+1-k)!}. \end{aligned}$$

REFERENCES

- [1] G. Montavon, S. Lapuschkin, A. Binder, W. Samek, and K.-R. Müller, "Explaining nonlinear classification decisions with deep Taylor decomposition," *Pattern Recognition*, vol. 65, pp. 211–222, May 2017. [Online]. Available: <https://linkinghub.elsevier.com/retrieve/pii/S0031320316303582>

- [2] S. Dutta, X. Chen, and S. Sankaranarayanan, "Reachability analysis for neural feedback systems using regressive polynomial rule inference," in *Proceedings of the 22nd ACM International Conference on Hybrid Systems: Computation and Control*. Montreal Quebec Canada: ACM, Apr. 2019, pp. 157–168. [Online]. Available: <https://dl.acm.org/doi/10.1145/3302504.3311807>
- [3] S. Obla, X. Gong, A. Aloufi, P. Hu, and D. Takabi, "Effective Activation Functions for Homomorphic Evaluation of Deep Neural Networks," *IEEE Access*, vol. 8, pp. 153 098–153 112, 2020. [Online]. Available: <https://ieeexplore.ieee.org/document/9169889/>
- [4] G. Lai, Z. Liu, Y. Zhang, and C. L. P. Chen, "Adaptive Position/Attitude Tracking Control of Aerial Robot With Unknown Inertial Matrix Based on a New Robust Neural Identifier," *IEEE Transactions on Neural Networks and Learning Systems*, vol. 27, no. 1, pp. 18–31, Jan. 2016. [Online]. Available: <http://ieeexplore.ieee.org/document/7061535/>
- [5] D. Nodland, H. Zargazadeh, and S. Jagannathan, "Neural Network-Based Optimal Adaptive Output Feedback Control of a Helicopter UAV," *IEEE Transactions on Neural Networks and Learning Systems*, vol. 24, no. 7, pp. 1061–1073, Jul. 2013. [Online]. Available: <http://ieeexplore.ieee.org/document/6487408/>
- [6] B. Xu, D. Wang, Y. Zhang, and Z. Shi, "DOB-Based Neural Control of Flexible Hypersonic Flight Vehicle Considering Wind Effects," *IEEE Transactions on Industrial Electronics*, vol. 64, no. 11, pp. 8676–8685, Nov. 2017.
- [7] A. P. Pope, J. S. Ide, D. Micovic, H. Diaz, D. Rosenbluth, L. Ritholtz, J. C. Twedt, T. T. Walker, K. Alcedo, and D. Javorsek, "Hierarchical Reinforcement Learning for Air-to-Air Combat," *arXiv:2105.00990 [cs]*, Jun. 2021, arXiv: 2105.00990. [Online]. Available: <http://arxiv.org/abs/2105.00990>
- [8] L. Shen, L. R. Margolies, J. H. Rothstein, E. Fluder, R. McBride, and W. Sieh, "Deep Learning to Improve Breast Cancer Detection on Screening Mammography," *Scientific Reports*, vol. 9, no. 1, p. 12495, Aug. 2019. [Online]. Available: <https://www.nature.com/articles/s41598-019-48995-4>
- [9] O.-A. Kwabena, Z. Qin, T. Zhuang, and Z. Qin, "MSCryptoNet: Multi-Scheme Privacy-Preserving Deep Learning in Cloud Computing," *IEEE Access*, vol. 7, pp. 29 344–29 354, 2019. [Online]. Available: <https://ieeexplore.ieee.org/document/8651459/>
- [10] "Hyperbolic tangent: Series representations (subsection 06/04)." [Online]. Available: <https://functions.wolfram.com/ElementaryFunctions/Tanh/06/04/>
- [11] C. Huang, J. Fan, W. Li, X. Chen, and Q. Zhu, "ReachNN: Reachability Analysis of Neural-Network Controlled Systems," *ACM Transactions on Embedded Computing Systems*, vol. 18, no. 5s, pp. 106:1–106:22, Oct. 2019. [Online]. Available: <https://doi.org/10.1145/3358228>
- [12] M. Vlček, "CHEBYSHEV POLYNOMIAL APPROXIMATION FOR ACTIVATION SIGMOID FUNCTION," *Neural Network World*, vol. 22, no. 4, pp. 387–393, 2012. [Online]. Available: <http://www.nnw.cz/obsahy12.html#22.023>
- [13] A. B. Koç and A. Kurnaz, "A new kind of double Chebyshev polynomial approximation on unbounded domains," *Boundary Value Problems*, vol. 2013, no. 1, p. 10, Dec. 2013. [Online]. Available: <https://boundaryvalueproblems.springeropen.com/articles/10.1186/1687-2770-2013-10>
- [14] B. K. Alpert and V. Rokhlin, "A Fast Algorithm for the Evaluation of Legendre Expansions," *SIAM Journal on Scientific and Statistical Computing*, vol. 12, no. 1, pp. 158–179, Jan. 1991. [Online]. Available: <https://epubs.siam.org/doi/abs/10.1137/0912009>
- [15] Y. Lee, J.-W. Lee, Y.-S. Kim, and J.-S. No, "Near-Optimal Polynomial for Modulus Reduction Using L2-Norm for Approximate Homomorphic Encryption," *IEEE Access*, vol. 8, pp. 144 321–144 330, 2020. [Online]. Available: <https://ieeexplore.ieee.org/document/9159551/>
- [16] D. Baptista and F. Morgado-Dias, "Low-resource hardware implementation of the hyperbolic tangent for artificial neural networks," *Neural Computing and Applications*, vol. 23, no. 3-4, pp. 601–607, Sep. 2013. [Online]. Available: <http://link.springer.com/10.1007/s00521-013-1407-x>
- [17] J.-W. Lee, E. Lee, Y. Lee, Y.-S. Kim, and J.-S. No, "High-precision bootstrapping of rms-ckks homomorphic encryption using optimal min-max polynomial approximation and inverse sine function," *Cryptology ePrint Archive, Report 2020/552*, 2020, <https://eprint.iacr.org/2020/552>.
- [18] Y. Lee, J. Lee, Y.-S. Kim, H. Kang, and J.-S. No, "High-precision approximate homomorphic encryption by error variance minimization," *Cryptology ePrint Archive, Report 2020/1549*, 2020, <https://eprint.iacr.org/2020/1549>.
- [19] H. Bateman, A. Erdélyi, Bateman Manuscript Project, and USA, Eds., *Higher transcendental functions*, ser. California Institute of Technology Bateman Manuscript Project. New York, NY: McGraw-Hill, 1953.
- [20] A. P. Engelbrecht, "Using the Taylor expansion of multilayer feedforward neural networks," *South African Computer Journal*, vol. 2000, no. 26, pp. 181–189, Nov. 2000. [Online]. Available: <https://journals.co.za/content/comp/2000/26/EJC27886>
- [21] X. Chen, Q. Ma, and T. Alkharobi, "New neural networks based on taylor series and their research," in *2009 2nd IEEE International Conference on Computer Science and Information Technology*, Aug 2009, pp. 291–294.
- [22] D. Balduzzi, B. McWilliams, and T. Butler-Yeoman, "Neural Taylor approximations: convergence and exploration in rectifier networks," in *Proceedings of the 34th International Conference on Machine Learning - Volume 70*, ser. ICML'17. Sydney, NSW, Australia: JMLR.org, Aug. 2017, pp. 351–360.
- [23] D. Guo, Z. Nie, and L. Yan, "Novel Discrete-Time Zhang Neural Network for Time-Varying Matrix Inversion," *IEEE Transactions on Systems, Man, and Cybernetics: Systems*, vol. 47, no. 8, pp. 2301–2310, Aug. 2017.
- [24] A. S. Gaikwad and M. El-Sharkawy, "Pruning convolution neural network (squeezeNet) using taylor expansion-based criterion," in *2018 IEEE International Symposium on Signal Processing and Information Technology (ISSPIT)*, Dec. 2018, pp. 1–5, iSSN: 2162-7843.
- [25] I. S. Gradshteyn, I. M. Ryzhik, and A. Jeffrey, *Table of integrals, series, and products*, 7th ed. Amsterdam ; Boston: Academic Press, 2007.
- [26] M. AboulAtta, M. Ossadnik, and S.-A. Ahmadi, "Stabilizing Inputs to Approximated Nonlinear Functions for Inference with Homomorphic Encryption in Deep Neural Networks," *arXiv:1902.01870 [cs, stat]*, Feb. 2019, arXiv: 1902.01870. [Online]. Available: <http://arxiv.org/abs/1902.01870>
- [27] R. Bojanic and M. Vuilleumier, "On the rate of convergence of Fourier-Legendre series of functions of bounded variation," *Journal of Approximation Theory*, vol. 31, no. 1, pp. 67–79, Jan. 1981. [Online]. Available: <https://linkinghub.elsevier.com/retrieve/pii/0021904581900319>
- [28] A. H. Namin, K. Leboeuf, R. Muscedere, H. Wu, and M. Ahmadi, "Efficient hardware implementation of the hyperbolic tangent sigmoid function," in *2009 IEEE International Symposium on Circuits and Systems*, May 2009, pp. 2117–2120, iSSN: 2158-1525.
- [29] A. Armato, L. Fanucci, E. Scilingo, and D. De Rossi, "Low-error digital hardware implementation of artificial neuron activation functions and their derivative," *Microprocessors and Microsystems*, vol. 35, no. 6, pp. 557–567, Aug. 2011. [Online]. Available: <https://linkinghub.elsevier.com/retrieve/pii/S0141933111000731>
- [30] G. Katz, D. A. Huang, D. Ibeling, K. Julian, C. Lazarus, R. Lim, P. Shah, S. Thakoor, H. Wu, A. Zeljić, D. L. Dill, M. J. Kochenderfer, and C. Barrett, "The Marabou Framework for Verification and Analysis of Deep Neural Networks," in *Computer Aided Verification*, ser. Lecture Notes in Computer Science, I. Dillig and S. Tasiran, Eds. Cham: Springer International Publishing, 2019, pp. 443–452.
- [31] M. Berz, "From Taylor series to Taylor models," in *Symposium on Nonlinear Dynamics*, Santa Barbara, California (USA), 1997, pp. 1–23. [Online]. Available: <http://aip.scitation.org/doi/abs/10.1063/1.53493>
- [32] —, "Taylor models and other validated functional inclusion methods," *International Journal of Pure and Applied Mathematics*, vol. 4, no. 4, pp. 379–456, 2003.
- [33] *IEEE Standard for Interval Arithmetic (Simplified)*, 2018.
- [34] H. Bateman, A. Erdelyi, W. Magnus, F. Oberhettinger, and F. G. Tricomi, *Integral Transforms*. New York: McGraw-Hill Book Company, 1954, vol. I.
- [35] "scikit-learn: machine learning in Python — scikit-learn 0.22.2 documentation." [Online]. Available: <https://scikit-learn.org/stable/>
- [36] "PyTorch." [Online]. Available: <https://www.pytorch.org>
- [37] "TensorFlow." [Online]. Available: <https://www.tensorflow.org/>
- [38] J. Misra and I. Saha, "Artificial neural networks in hardware: A survey of two decades of progress," *Neurocomputing*, vol. 74, no. 1-3, pp. 239–255, Dec. 2010. [Online]. Available: <https://linkinghub.elsevier.com/retrieve/pii/S092523121000216X>
- [39] D. Maliuk and Y. Makris, "An Experimentation Platform for On-Chip Integration of Analog Neural Networks: A Pathway to Trusted and Robust Analog/RF ICs," *IEEE Transactions on Neural Networks and Learning Systems*, vol. 26, no. 8, pp. 1721–1734, Aug. 2015. [Online]. Available: <http://ieeexplore.ieee.org/lpdocs/epic03/wrapper.htm?arnumber=6901256>
- [40] A. M. Abdelsalam, J. M. P. Langlois, and F. Cheriet, "Accurate and Efficient Hyperbolic Tangent Activation Function on FPGA using the

- DCT Interpolation Filter,” *arXiv:1609.07750 [cs]*, Sep. 2016, arXiv:1609.07750. [Online]. Available: <http://arxiv.org/abs/1609.07750>
- [41] C. D. Schuman, T. E. Potok, R. M. Patton, J. D. Birdwell, M. E. Dean, G. S. Rose, and J. S. Plank, “A Survey of Neuromorphic Computing and Neural Networks in Hardware,” *arXiv:1705.06963 [cs]*, May 2017, arXiv:1705.06963. [Online]. Available: <http://arxiv.org/abs/1705.06963>
- [42] H. J. Sussmann, “Uniqueness of the weights for minimal feedforward nets with a given input-output map,” *Neural Networks*, vol. 5, no. 4, pp. 589–593, Jul. 1992. [Online]. Available: <https://linkinghub.elsevier.com/retrieve/pii/S0893608005800371>
- [43] F. Albertini and E. D. Sontag, “Uniqueness of Weights for Neural Networks,” in *Artificial Neural Networks for Speech and Vision*. Chapman and Hall, London, 1993, pp. 113–125.
- [44] C. DiMattina and K. Zhang, “How to Modify a Neural Network Gradually Without Changing Its Input-Output Functionality,” *Neural Computation*, vol. 22, no. 1, pp. 1–47, Jan. 2010. [Online]. Available: <http://www.mitpressjournals.org/doi/10.1162/neco.2009.05-08-781>
- [45] F. Tramèr, F. Zhang, A. Juels, M. K. Reiter, and T. Ristenpart, “Stealing machine learning models via prediction apis,” in *Proceedings of the 25th USENIX Conference on Security Symposium*, ser. SEC’16. USA: USENIX Association, 2016, p. 601–618.
- [46] N. Papernot, P. McDaniel, I. Goodfellow, S. Jha, Z. B. Celik, and A. Swami, “Practical Black-Box Attacks against Machine Learning,” in *Proceedings of the 2017 ACM on Asia Conference on Computer and Communications Security - ASIA CCS ’17*. Abu Dhabi, United Arab Emirates: ACM Press, 2017, pp. 506–519. [Online]. Available: <http://dl.acm.org/citation.cfm?doid=3052973.3053009>
- [47] S. J. Oh, B. Schiele, and M. Fritz, *Towards Reverse-Engineering Black-Box Neural Networks*. Cham: Springer International Publishing, 2019, pp. 121–144. [Online]. Available: https://doi.org/10.1007/978-3-030-28954-6_7
- [48] V. Duddu, D. Samanta, D. V. Rao, and V. E. Balas, “Stealing neural networks via timing side channels,” *ArXiv*, vol. abs/1812.11720, 2018.
- [49] T. Orekondy, B. Schiele, and M. Fritz, “Knockoff Nets: Stealing Functionality of Black-Box Models,” in *2019 IEEE/CVF Conference on Computer Vision and Pattern Recognition (CVPR)*. Long Beach, CA, USA: IEEE, Jun. 2019, pp. 4949–4958. [Online]. Available: <https://ieeexplore.ieee.org/document/8953839>
- [50] S. Dutta, S. Jha, S. Sankaranarayanan, and A. Tiwari, “Output Range Analysis for Deep Feedforward Neural Networks,” in *NASA Formal Methods*, ser. Lecture Notes in Computer Science, A. Dutle, C. Muñoz, and A. Narkawicz, Eds. Cham: Springer International Publishing, 2018, pp. 121–138.
- [51] B. Darvish Rouani, M. Samragh, T. Javidi, and F. Koushanfar, “Safe Machine Learning and Defeating Adversarial Attacks,” *IEEE Security & Privacy*, vol. 17, no. 2, pp. 31–38, Mar. 2019. [Online]. Available: <https://ieeexplore.ieee.org/document/8677311>
- [52] A. Venzke and S. Chatzivasileiadis, “Verification of Neural Network Behaviour: Formal Guarantees for Power System Applications,” *arXiv:1910.01624 [cs, math]*, Jan. 2020, arXiv:1910.01624. [Online]. Available: <http://arxiv.org/abs/1910.01624>
- [53] W. Xiang, H.-D. Tran, and T. T. Johnson, “Output Reachable Set Estimation and Verification for Multilayer Neural Networks,” *IEEE Transactions on Neural Networks and Learning Systems*, vol. 29, no. 11, pp. 5777–5783, Nov. 2018. [Online]. Available: <https://ieeexplore.ieee.org/document/8318388/>
- [54] K. Dvijotham, R. Stanforth, S. Gowal, C. Qin, S. De, and P. Kohli, “Efficient neural network verification with exactness characterization,” in *UAI*, 2019.
- [55] C. Liu, T. Arnon, C. Lazarus, C. W. Barrett, and M. J. Kochenderfer, “Algorithms for verifying deep neural networks,” *ArXiv*, vol. abs/1903.06758, 2019.
- [56] R. R. Bunel, I. Turkaslan, P. Torr, P. Kohli, and P. K. Mudigonda, “A unified view of piecewise linear neural network verification,” in *Advances in Neural Information Processing Systems 31*, S. Bengio, H. Wallach, H. Larochelle, K. Grauman, N. Cesa-Bianchi, and R. Garnett, Eds. Curran Associates, Inc., 2018, pp. 4790–4799. [Online]. Available: <http://papers.nips.cc/paper/7728-a-unified-view-of-piecewise-linear-neural-network-verification.pdf>
- [57] T. Gehr, M. Mirman, D. Drachler-Cohen, P. Tsankov, S. Chaudhuri, and M. Vechev, “AI2: Safety and Robustness Certification of Neural Networks with Abstract Interpretation,” in *2018 IEEE Symposium on Security and Privacy (SP)*, May 2018, pp. 3–18, iSSN: 2375-1207.
- [58] C. Huang, J. Fan, X. Chen, W. Li, and Q. Zhu, “Divide and Slide: Layer-Wise Refinement for Output Range Analysis of Deep Neural Networks,” *IEEE Transactions on Computer-Aided Design of Integrated Circuits and Systems*, vol. 39, no. 11, pp. 3323–3335, Nov. 2020.
- [59] H. D. Tran, X. Yang, D. M. Lopez, P. Musau, L. V. Nguyen, W. Xiang, S. Bak, and T. T. Johnson, “NNV: The Neural Network Verification Tool for Deep Neural Networks and Learning-Enabled Cyber-Physical Systems,” in *Computer Aided Verification - 32nd International Conference, CAV 2020, Proceedings*. Springer, 2020, pp. 3–17. [Online]. Available: <https://augusta.pure.elsevier.com/en/publications/nnv-the-neural-network-verification-tool-for-deep-neural-networks>
- [60] H.-D. Tran, P. Musau, D. Manzananas Lopez, X. Yang, L. V. Nguyen, W. Xiang, and T. T. Johnson, “Parallelizable Reachability Analysis Algorithms for Feed-Forward Neural Networks,” in *2019 IEEE/ACM 7th International Conference on Formal Methods in Software Engineering (FormaliSE)*. Montreal, QC, Canada: IEEE, May 2019, pp. 51–60. [Online]. Available: <https://ieeexplore.ieee.org/document/8807491/>
- [61] S. YAGHOUBI and G. FAINEKOS, “Worst-case Satisfaction of STL Specifications Using Feedforward Neural Network Controllers: A Lagrange Multipliers Approach,” in *2020 Information Theory and Applications Workshop (ITA)*, Feb. 2020, pp. 1–20, iSSN: 2642-7338.
- [62] R. Ivanov, J. Weimer, R. Alur, G. J. Pappas, and I. Lee, “Verisig: verifying safety properties of hybrid systems with neural network controllers,” in *Proceedings of the 22nd ACM International Conference on Hybrid Systems: Computation and Control*, ser. HSCC ’19. Montreal, Quebec, Canada: Association for Computing Machinery, Apr. 2019, pp. 169–178. [Online]. Available: <https://doi.org/10.1145/3302504.3311806>
- [63] X. Huang, D. Kroening, W. Ruan, J. Sharp, Y. Sun, E. Thamo, M. Wu, and X. Yi, “A survey of safety and trustworthiness of deep neural networks: Verification, testing, adversarial attack and defence, and interpretability,” *Computer Science Review*, vol. 37, p. 100270, Aug. 2020. [Online]. Available: <https://linkinghub.elsevier.com/retrieve/pii/S1574013719302527>
- [64] T. Wu, Y. Dong, Z. Dong, A. Singa, X. Chen, and Y. Zhang, “Testing Artificial Intelligence System Towards Safety and Robustness: State of the Art,” *IAENG International Journal of Computer Science*, vol. 47, no. 3, Sep. 2020.
- [65] A. Laakso and G. Cottrell, “Content and cluster analysis: Assessing representational similarity in neural systems,” *Philosophical Psychology*, vol. 13, no. 1, pp. 47–76, Mar. 2000. [Online]. Available: <http://www.tandfonline.com/doi/abs/10.1080/09515080050002726>
- [66] Y. Li, J. Yosinski, J. Clune, H. Lipson, and J. Hopcroft, “Convergent Learning: Do different neural networks learn the same representations?” in *Journal of Machine Learning Research Conference Proceedings*, 2015, pp. 196–212.
- [67] M. Raghu, J. Gilmer, J. Yosinski, and J. Sohl-Dickstein, “Svcca: Singular vector canonical correlation analysis for deep learning dynamics and interpretability,” in *Advances in Neural Information Processing Systems 30*, I. Guyon, U. V. Luxburg, S. Bengio, H. Wallach, R. Fergus, S. Vishwanathan, and R. Garnett, Eds. Curran Associates, Inc., 2017, pp. 6076–6085. [Online]. Available: <http://papers.nips.cc/paper/7188-svcca-singular-vector-canonical-correlation-analysis-for-deep-learning-dynamics-and-interpretability.pdf>
- [68] A. Morcos, M. Raghu, and S. Bengio, “Insights on representational similarity in neural networks with canonical correlation,” in *Advances in Neural Information Processing Systems 31*, S. Bengio, H. Wallach, H. Larochelle, K. Grauman, N. Cesa-Bianchi, and R. Garnett, Eds. Curran Associates, Inc., 2018, pp. 5727–5736. [Online]. Available: <http://papers.nips.cc/paper/7815-insights-on-representational-similarity-in-neural-networks-with-canonical-correlation.pdf>
- [69] S. Kornblith, M. Norouzi, H. Lee, and G. Hinton, “Similarity of Neural Network Representations Revisited,” in *Proceedings of the 36th International Conference on Machine Learning*, Long Beach, CA, USA, 2019.
- [70] C.-H. Chang, “Deep and Shallow Architecture of Multilayer Neural Networks,” *IEEE Transactions on Neural Networks and Learning Systems*, vol. 26, no. 10, pp. 2477–2486, Oct. 2015. [Online]. Available: <http://ieeexplore.ieee.org/document/7010967/>
- [71] H. Huang and H. Yu, “LTNN: A Layerwise Tensorized Compression of Multilayer Neural Network,” *IEEE Transactions on Neural Networks and Learning Systems*, vol. 30, no. 5, pp. 1497–1511, May 2019. [Online]. Available: <https://ieeexplore.ieee.org/document/8480873/>
- [72] M. I. Qureshi, S. Porwal, D. Ahamad, and K. A. Quraishi, “Successive differentiations of tangent, cotangent, secant, cosecant functions and related hyperbolic functions (A hypergeometric approach),” *International Journal of Mathematics Trends and Technology*, vol. 65, no. 7, pp. 325–367, Jul. 2019. [Online]. Available: <http://www.ijmtjournal.org/archive/ijmtt-v65i7p541>